Supplementary Data

Treatment of invasive brain tumors using a chain-like nanoparticle

Pubudu M. Peiris[1,2,3], Aaron Abramowski[3,4], James Mcginnity[1,3], Elizabeth Doolittle[1,2,3], Randall Toy[1,2,3], Ramamurthy Gopalakrishnan[2,3], Shruti Shah[1,3], Lisa Bauer[2,3,5], Ketan B. Ghaghada[6,7], Christopher Hoimes[8,9], Susann M. Brady-Kalnay[9,10], James P. Basilion[1,2,3,9], Mark A. Griswold[2,3,9], and Efstathios Karathanasis[1,2,3,9*]

[1] Department of Biomedical Engineering, Case Western Reserve University, Cleveland, Ohio
[2] Department of Radiology, Case Western Reserve University, Cleveland, Ohio
[3] Case Center for Imaging Research, Case Western Reserve University, Cleveland, Ohio
[4] Department of Biochemistry, Case Western Reserve University, Cleveland, Ohio
[5] Department of Physics, Case Western Reserve University, Cleveland, Ohio
[6] Edward B. Singleton Department of Pediatric Radiology, Texas Children's Hospital, Houston, Texas
[7] Department of Radiology, Baylor College of Medicine, Houston, Texas
[8] University Hospitals Case Medical Center, Cleveland, Ohio
[9] Case Comprehensive Cancer Center, Case Western Reserve University, Cleveland, Ohio
[10] Department of Molecular Biology and Microbiology, Case Western Reserve University, Cleveland, Ohio

[*] Email: stathis@case.edu

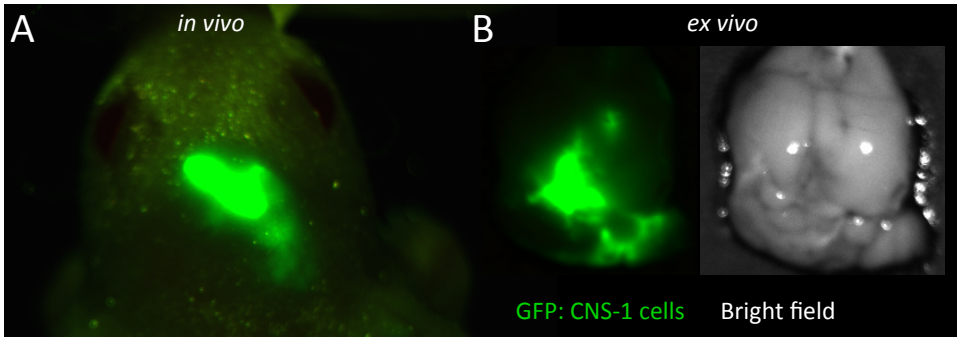

Supplementary Fig. S1. Representative *in vivo* and *ex vivo* images using a Maestro FLEX *In Vivo* Imaging System. A, fluorescence imaging was performed *in vivo* with Maestro system using a filter appropriate for GFP fluorescence. The location of the tumor in the brain is indicated in green, since the tumor cells were expressing GFP. B, *ex vivo* fluorescence imaging of the whole brain of the same animal is shown (left panel). Animals were sacrificed, and the brain was excised and imaged using the Maestro System. The bright field image of the same brain is also shown (right panel). Due to the emission of GFP in the green zone of the visible spectrum, the depth-dependent attenuation of the fluorescence signal by the brain tissues and the skull does not allow accurate quantification of the number of CNS-1 glioma cells *in vivo* in the case of *in vivo* imaging.

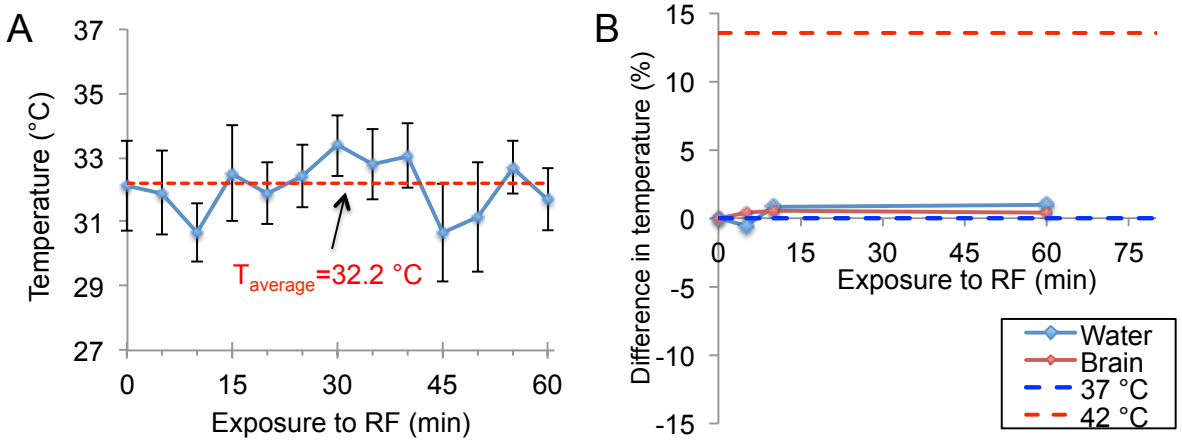

Supplementary Fig. S2. Effect of the RF field on the temperature of brain tissues. A, The effect of the RF field on the temperature of the brain tumor was measured in the orthotopic CNS-1 glioma model in mice (n=3). Following IV injection of the nanochain particle, the RF field was applied following an identical protocol to the one used during therapies. A LumaSense Luxtron m3300 Fluoroptic thermometer probe was used to monitor the temperature of the tumor region. Using a stereotaxic rodent frame, the tip of the temperature probe was then inserted in the tumor region by using the original coordinates of tumor inoculation (AP= +0.5 and ML= - 2.0 from bregma in the right striatum at a depth of -3 mm from dura). The temperature was measured for a 60-min application of the RF, while the animal was under anesthesia. B, a similar experiment was performed *ex vivo*. Whole brains were retrieved from healthy animals (n=3) and placed in vial with 1.8 mL saline solution. Temperature of saline and brain tissue was measured using an Omega Type T hypo needle thermometer. Using a water bath, the temperature of saline was elevated and kept at 37 °C. Once the temperature of the brain equilibrated at 37 °C, the vial was exposed to the RF field for 60 min using the same custom-made solenoid coil used for the animal studies (amplitude B=5 mT, frequency f=10 kHz). Starting at 37 °C at t=0 (ΔT=0%; blue dotted line), the relationship of ΔT of the saline solution and brain to RF exposure for 60 min was recorded. As an indication of significant temperature increase, the ΔT for 42 °C is provided (ΔT=13.5%, red dotted line).

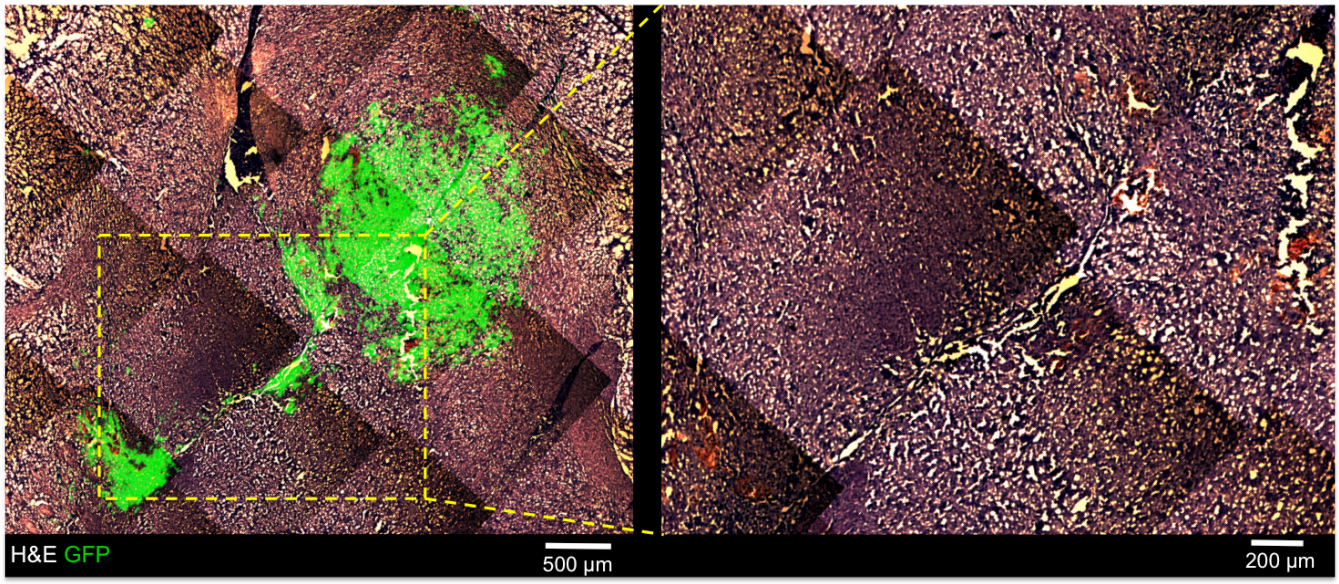

Supplementary Fig. S3. Bright field microscopy and fluorescence was performed on an entire histological section of the brain stained with Hematoxylin-Eosin (green: CNS-1 glioma cells (GFP)). The same histological section shown in Fig. 4A was used (left panel). Higher magnification of the same section shows the H&E stain of an invasive site (right panel).

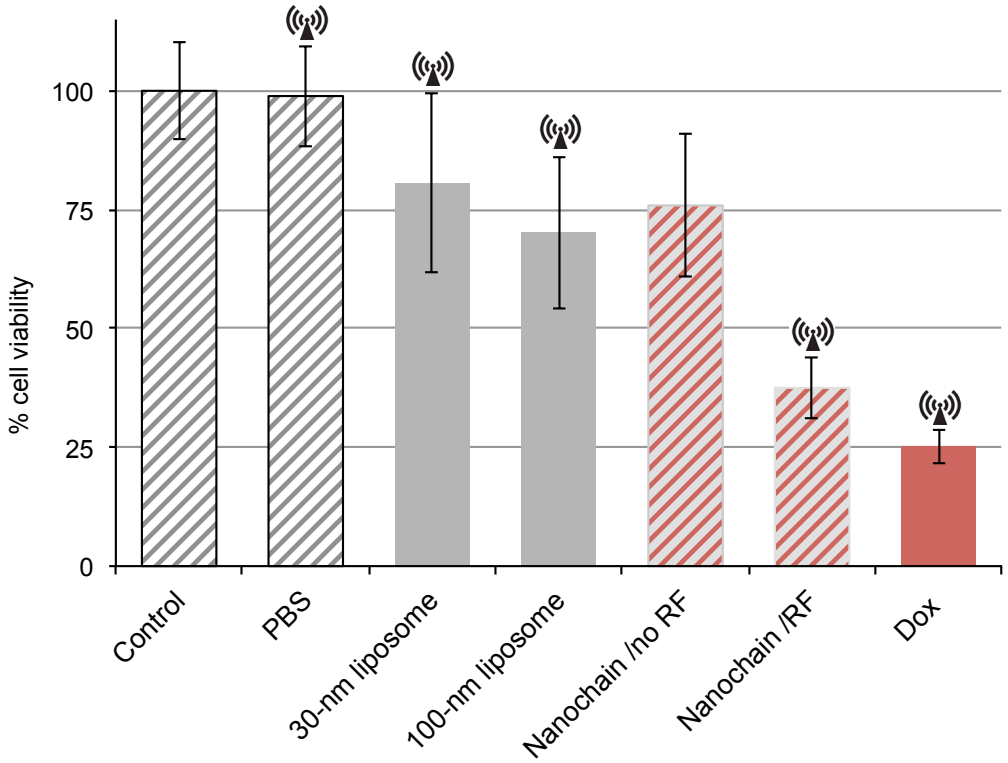

Supplementary Fig. S4. Cytotoxicity of nanochain particles on CNS-1 cells. Cell viability was used as an indication of the cytotoxic effects of nanochains (with or without RF) on CNS-1 cancer cells at 100 µM DOX. Control treatments included free DOX, and 30-nm and 100-nm liposomal DOX. The cells were seeded at a density of 10^5 cells/well in a 6-well plate 24 h before incubation with the formulations. Cells were incubated with the treatment for 180 minutes at a concentration of 100 µM DOX per well. The cells were washed three times with fresh medium and incubated for 48 h at 37°C and 5% CO_2 in a

humidified environment. The number of viable cells was determined using a formazan-based cell counting assay (CCK-8). Untreated cells were served as live controls for normalization of the data.

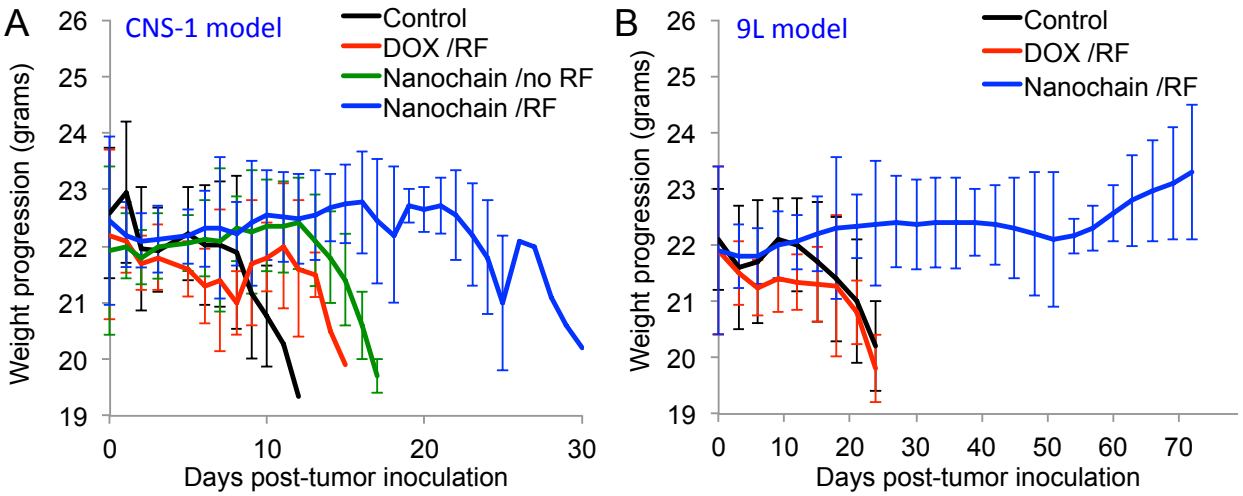

Supplementary Fig. S5. Weight progression of animals bearing orthotopic (A) CNS-1 or (B) 9L glioma tumors after DOX treatments. All formulations were administered at a dose of 0.5 mg DOX per kg b.w. Each treatment was administered three times at day 5, 7 and 9 after tumor inoculation. In the case of treatments combined with the RF field, animals were exposed for 60 min to an RF field (amplitude B=5 mT, frequency f=10 kHz) using a custom-made solenoid coil. The average weight progression of the glioma-bearing animals is shown after treatment with saline (control), DOX followed by RF, and nanochains with or without RF (n=5 mice in each group). The survival times of these groups is shown Fig. 5.